Robustness of Hill's overlapping-generation method for calculating N_e to extreme violations of model assumptions

Robin S. Waples

School of Aquatic and Fishery Sciences, University of Washington, Seattle

Key words: population genetics, computer simulations, reproductive skew, effective population size, autocorrelation, covariance

Word count: 5741 (main text)

Corresponding author:
Robin Waples (robinw3@uw.edu, (206) 789-4648)

February 2023

Abstract

For species with overlapping generations, the most widely-used method to calculate effective population size (N_e) is Hill's, the key parameter for which is lifetime variance in offspring number ($V_{k\bullet}$). Hill's model makes two general assumptions: 1) stable size and age structure; 2) independence of reproduction and survival over time. Previous work has evaluated assumption 1; this study evaluates the independence assumptions. Genetic drift (loss of heterozygosity and increase in allele-frequency variance) was simulated in age-structured populations using methods that: met Hill's assumptions (Option 1); or created strong positive (Option 2) or strong negative (Option 3) temporal autocorrelations in reproduction and covariances between reproduction and survival. Compared to Option 1, Options 2 and 3 led to greatly elevated or reduced $V_{k\bullet}$, and hence greatly reduced or elevated N_e, respectively. A new index is introduced ($\rho_{\alpha,\alpha+}$), which is the correlation between 1) the number of offspring produced by each individual at the age at maturity (α), and 2) the total number of offspring produced during the rest of their lifetimes. Mean $\rho_{\alpha,\alpha+}$ was ≈0 under Option 1, strongly positive under Option 2, and strongly negative under Option 3. Despite the dramatic violations of Hill's independence assumptions in Options 2 and 3, when $V_{k\bullet}$ was calculated from the realized population pedigree and used to calculate N_e in Hill's model, the result accurately predicted the rate of genetic drift in simulated populations. These results held for scenarios where age-specific reproductive skew was random (variance≈mean) and highly overdispersed (variance up to 20 times the mean). Collectively, these results are good new for researchers as they demonstrate the robustness of Hill's model to very strong violations of model assumptions.

INTRODUCTION

The majority of populations in nature are age structured, but most evolutionary theory was originally developed for models that assume discrete generations. Considerable progress has been made in adapting discrete-generation theory to account for age structure (e.g., Charlesworth 1994; Cushing et al. 1994; Lande et al. 2003), but this process remains challenging.

One of the most important parameters in evolutionary biology is effective population size (N_e), which, in addition to determining the rate of genetic drift, modulates the effectiveness of natural selection and hence the rate of evolutionary adaptation. Wright's original concept of N_e (1931, 1938) assumed that generates were discrete. Of the various methods researchers have proposed for incorporating age structure into the concept of effective size, that of Hill (1972) is the most widely used. Hill showed that, if age-structure is stable and the population produces a constant number (N_1) of offspring in each cohort, N_e per generation is given by

$$N_e \approx \frac{4N_1T}{V_{k\bullet}+2} \quad , \qquad (1)$$

where $T=\Sigma x l_x b_x / \Sigma l_x b_x$ is generation length (average age of parents of the newborn cohort) and $V_{k\bullet}$ is the variance in lifetime reproductive success (*LRS*), measured as the variance in lifetime number of offspring among the N_1 individuals in a cohort. In his derivation, Hill assumed that an individual's reproductive output in one time period does not affect either its reproduction or survival in any subsequent time period; that is, his model assumed no temporal autocorrelation in reproduction, and no covariance of reproduction and subsequent survival.

The assumption in Hill's model of stable age structure and constant N has been extensively evaluated with diverse life histories and found to be robust to random demographic variability (Waples et al. 2011; 2014). However, the models used in those evaluations assumed independence of reproduction and survival, and the robustness of Hill's model to his assumptions of no temporal autocorrelation in reproduction and no covariance of reproduction and survival has not been rigorously tested. This is an important gap, for two major reasons.

First, temporal autocorrelations and covariances are common in many species. The theory of life-history evolution is based on the premise that biological constraints impose intrinsic tradeoffs between reproduction now and reproduction later, and between reproduction and subsequent survival (Williams 1966; Bell 1980; Reznick 1992; Roff 1992). These tradeoffs

imply a negative temporal autocorrelation in individual reproduction and a negative covariance between reproduction and survival. In the real world, however, the opposite patterns also can be found, and these patterns can be explained (and even expected) when one accepts the possibility that individuals are not interchangeable (van Noordwijk and de Jong 1986). Persistent individual differences in reproductive success (Lee et al. 2011) are generally taken to reflect individual differences in 'quality', which is a rather slippery concept but is generally thought to be positively correlated with fitness (Wilson and Nussey 2010). Individual differences in quality can be influenced by both genetic and environmental factors (Byholm et al. 2007) and can persist across many reproductive seasons [e.g., owing to long-lasting maternal effects (Mousseau and Fox 1998; Kruuk 2004) or mating dynamics (McElligot et al. 2000; Pelletier et al. 2006)]. In species for which fecundity increases with age (as applies to most ectotherms with indeterminate growth), persistent individual differences are likely the rule rather than the exception: individuals that are large for their age early in life will generally have relatively high reproductive success, and they also are likely to be large for their age in later years (Waples and Feutry 2022). Likewise, if individual quality is high for both reproduction and survival, that can offset any costs of reproduction and lead to a positive covariance (Smith 1981; Pelletier et al. 2006), a result that also can occur if mortality is anthropogenically modulated (e.g., if hunters avoid killing female moose with calves; Lee et al. 2020).

The second factor is that although monitoring evolutionary dynamics in age-structured populations remains logistically challenging, especially for long-lived species, the recent genomics revolution has greatly increased our ability to reconstruct population pedigrees using non-invasive genetic samples. Consider, then, the following scenario:

- A researcher is conducting a long-term pedigreed study of their focal species;
- The pedigree data are sufficient to robustly estimate generation length and variance in *LRS;*
- The biology of the focal species is such that it generates substantial autocorrelation of reproductive success and/or covariance of reproduction and survival.

A key question then becomes, "If the empirical estimates of T and $V_{k_\bullet}$ are used in Equation 1 to estimate N_e, will the result accurately reflect the rate of genetic drift in the population, even though some of the key assumptions used to derive Equation 1 are strongly violated?"

The goal of this study is to answer this question. Using hypothetical vital rates for populations with overlapping generations, multi-year population pedigrees are simulated that a) conform to the independence assumptions of Hill's model (Option 1); b) generate strong positive autocorrelations and covariances (Option 2); and c) generate strong negative autocorrelations and covariances (Option 3). Along each pedigree, genetic variation is tracked at a number of loci, and the rates of genetic drift are quantified by two common metrics: rate of decline in heterozygosity, and rate of increase in allele frequency variance. These observed rates are compared with expected rates based on N_e calculated from the population pedigree using Hill's method (Equation 1).

METHODS

Population demography

The core evaluations modeled reproduction and genetic change in a hypothetical population with age at maturity α=3 and maximum age ω=10, which produced a maximum adult lifespan of AL=8 years (ages 3-10, inclusive; see core vital rates in Table 1). Population dynamics followed the discrete time, birth-pulse model of Caswell (2001), where individuals that reach age x produce on average b_x offspring and then survive to age x+1 with probability s_x. Because previous work had evaluated sensitivity to the constant-size assumption, to limit the number of potentially confounding variables, age structure was fixed and defined by the vector of cumulative survival through age x, l_x. Offspring were enumerated at age 1, so setting l_1=1 and letting N_1 be the number of offspring in each cohort that reach age 1, the numbers in each successive age class (x=2,ω) are given by N_x=$N_1 l_x$. For the core life table in Table 1, N_1=200 and the full vector of age-class abundance was (rounded to the nearest integer): N_x=[200,140,98,69,48,34,24,16,12,8]. Total abundance was ΣN_x=649, of which 340 were juveniles, so the adult census size was N_{Adult} = 309. These numbers apply to a single sex; sex ratio was 1:1 in the core analyses, so total population size was twice as large.

The core life table allowed patterns of age-specific fecundity and reproductive skew to differ between the sexes. In all analyses, fecundity was constant with age in females and reproduction followed a Poisson process (all ϕ=1), so every year all females behaved like a single Wright-Fisher population with essentially random variation in offspring number. In males, three scenarios were considered. In Scenario 1, b_x and ϕ_x were identical to values for

females. In Scenario 2, fecundity for males was proportional to age, and reproductive skew was moderately strong (for all ages ϕ_x=5, indicating that variance in offspring number was 5 times the mean). In Scenario 3, male b_x was also proportional to age, and reproductive skew was very strong (all ϕ_x=20). Fecundities were scaled to values that would produce a stable population by ensuring that $\Sigma b_x l_x$=2. With fecundities so scaled, the expected number of offspring produced in each time period by each age class within each sex was $B_x=b_xN_x$, with $\Sigma B_x=2N_1$=400 total offspring, of which half are male and half female.

Modeling reproduction

Two algorithms were used to ensure that the distribution of offspring number closely approximated the parametric values in the life table. *THEWEIGHT* (Waples 2020, 2022a) is a generalized Wright-Fisher model that allows for unequal parental expectations of reproductive success, specified by a vector of parental weights, $\boldsymbol{W}$. For a given set of b_x, N_x, and ϕ_x values, *THEWEIGHT* randomly generates a vector of parental weights that on average will produce the desired level of reproductive skew. Under Scenario 1, all weights were equal so the model simplified to the standard Wright-Fisher model. For Scenarios 2 and 3 in males, random $\boldsymbol{W}$ vectors were repeatedly generated until one was found with a coefficient of variation within a specified threshold (generally a few percent) of the target (see Waples 2022a for details). A convenient feature of *THEWEIGHT* is that it allows the user to simulate exactly the target number of offspring by randomly choosing parents for each offspring, with probabilities determined by $\boldsymbol{W}$. For each age of the adult lifespan, a pool of potential parents of the respective age was assembled, and from this pool B_x parental IDs were drawn, with replacement. This process was continued until a list of 400 parental IDs had been chosen. This process was then repeated for the opposite sex, and both resulting lists were randomized before combining them to specify both parents for each offspring in the new cohort.

The second algorithm (*NEGBINOM*) used a more traditional negative-binomial simulator to generate random vectors of offspring numbers ($\boldsymbol{k}$) expected to have the desired mean and variance. A disadvantage of this approach is that the realized mean of the simulated distribution is a random variable. As a consequence, the total number of offspring produced ($\Sigma\boldsymbol{k}$) also varies randomly and only by chance equals the target number. To maintain a constant total number of offspring in each cohort, the following procedure was used:

- For each age x, the *rnbinom* function in R was used to generate N_x random k values, using the parameterization $mu=b_x$ and $size=b_x^2/(V_{k(x)}-b_x)$, with $V_{k(x)}=\phi_x b_x$. Note that this function requires $V_{k(x)}>b_x$, so for Scenario 1 with $V_{k(x)}=b_x$ the *rpois* function was used instead.
- The total length of all the age-specific $\boldsymbol{k}$ vectors was compared with the target cohort size $= 2N_1$. This process was repeated until the total length fell in the range $[2N_1, 1.05*2N_1]$. At that point, the vectors of offspring numbers were converted to a list of parental IDs and this list was randomly downsampled (if necessary) to reach exactly $2N_1$ offspring.
- This entire process was repeated for the opposite sex.

The focus here is on scenarios that violate the assumptions of the Hill model that reproduction and survival are uncorrelated over time. Two related issues require consideration:

1) Does reproduction in one time period affect reproduction in any subsequent time period?
2) Does reproduction in one time period affect the probability of survival to subsequent time periods?

To see the consequences of a positive answer to either of these questions, note that the expected lifetime reproductive success [$E(k\bullet)$] of an individual is a simple additive function of its age-specific fecundity and its age at death (q):

$$E\left(k\bullet_q\right) = \sum_{x=1}^{q} E(k_x) = \sum_{x=1}^{q} b_x \quad . \qquad (2)$$

The variance of a sum, however, also depends on the covariance structure of the terms being added: var(A+B)=var(A)+var(B)+2cov(A,B). More generally, when applied to the variance of a sum of q terms:

$$var\left(k\bullet_q\right) = var(k_1) + var(k_2) + \cdots var\left(k_q\right) + 2\sum_{j<k}^{q} cov(k_j, k_k).$$

Since $var(k_x) = \phi_x b_x$, the above can be written as

$$var\left(k\bullet_q\right) = \phi_1 b_1 + \phi_2 b_2 + \cdots \phi_q b_q + 2\sum_{j<k}^{q} cov(k_j, k_k). \qquad (3)$$

The *AGENE* model (Waples et al. 2011) calculates $V_{k\bullet}$ and N_e using age-specific vital rates from an expanded life table and by adopting the Hill-Felsenstein assumption that expected values of all these covariance terms are zero.

Developing analytical expectations for these covariance terms under more realistic assumptions is not a simple task, especially in any generalized form. However, both of the algorithms described above can be tweaked to generate positive or negative correlations in reproductive success. The two algorithms do this in slightly different ways, and these

differences can be illustrated with a simple framework for calculation of *LRS* (Table 2). In this hypothetical example, reproductive success of a cohort of 20 individuals is tracked for a 5-year maximum lifespan. *NA*s in the table indicate individuals that were not alive at the specified age. In this example, 8 individuals died after age 1 and before reaching age 2, 4 died after age 2, and 3 each died after ages 3 and 4, leaving just 2 individuals that survived to age 5. Fecundity increased linearly with age (b_x = [1,2,3,4,5]), and the within-age variance was 5 times the mean (ϕ=5) for each age. To populate the table, vectors of offspring numbers were randomly generated for each age using the *rnbinom* function in R (R core team 2022) (generating 20 random values for age 1 with mean = 1 and variance = 5; 12 random values for age 2 with mean = 2 and variance = 10; etc.).

Results of one random realization of this process are shown in the left side of Table 2. At age 1, 2 individuals produced exactly 1 offspring, single individuals produced 2,3,5, and 6 offspring each, and the remaining 14 individuals produced no offspring. The '*LRS*' column shows that across the original cohort, lifetime offspring number ranged from 0 (6 individuals) to 31 (individual 5). Three factors contribute to the variance in *LRS* in this example. 1) Individuals that (by luck or pluck) survive to older ages have more opportunities to add to their *LRS*. 2) Because fecundity increases with age in this example, longer-lived individuals get an additional bonus because their reproductive success is higher in later years. 3) Variance in reproductive success is overdispersed within each age (ϕ>1). Collectively, these factors cause lifetime $V_{k\bullet}$ (58.1) to be much higher than the mean (4.85). So far, this example has followed the assumption of the Hill-Felsenstein model that there are no systematic correlations between individual reproductive success over time. We refer to this as Option 1.

Temporal correlations in reproductive success are easy to generate by sorting the randomly-generated vectors of offspring number before mapping them to individuals. The right side of Table 2 shows the results of sorting the $\boldsymbol{k}$ vector for each age such that the largest value is assigned to individual 1, the next largest to individual 2, and so on. This simple ploy accomplishes two things: 1) It creates persistent individual differences in reproductive success, which manifest as positive correlations between an individual's reproductive output across time; 2) It creates positive correlations between reproduction and subsequent survival, which enhance the strength of the persistent individual differences. This is Option 2. The net result is that $V_{k\bullet}$ more than doubles (to 122.9) while the mean remains the same.

In empirical datasets, the pairwise covariance terms can be challenging to deal with because a) they are very numerous for long-lived species, and b) sample sizes are generally small for comparisons involving older age classes. Here a new metric is introduced ($\rho_{\alpha,\alpha+}$) that generally can be applied to all individuals in a cohort that reach age at maturity. This metric represents the Pearson correlation coefficient between two vectors: $\boldsymbol{k_\alpha}$ = offspring number for all individuals at the age at first reproduction (α), and $\boldsymbol{k_{\alpha+}} = LRS - \boldsymbol{k_\alpha}$ = lifetime reproductive success of the same individuals for all subsequent years. In the example for Option 1 in Table 2, this correlation is slightly positive ($\rho_{\alpha,\alpha+}$=0.14) but not significantly so (P>0.5 for a two-tailed test). For the extreme Option 2, in contrast, this correlation was close to unity ($\rho_{\alpha,\alpha+}$=0.96; P<0.001).

Negative temporal correlations in reproductive success are easy to generate by reversing the sorting process and assigning the largest k value each year to the individual with the highest ID number (Option 3; see Figure S1). Since individuals with the highest ID numbers are the ones that die each year after reproduction, this ensures that new individuals get to reproduce each year, which in turn reduces $V_{k\bullet}$. Applying Option 3 to the simulated data in Table 2 reduced $V_{k\bullet}$ sharply (to 17.4) and led to a significantly negative correlation ($\rho_{\alpha,\alpha+}$=-0.43; P<0.05; Table S1).

Simulations using *THEWEIGHT* followed procedures described above, with one difference: at each age, instead of generating a random vector of offspring numbers, a random vector of parental weights was generated. In Option 1, the weights were assigned randomly to surviving individuals; otherwise, the weights were first sorted either largest-to-smallest (Option 2) or smallest-to-largest (Option 3) before assigning to survivors. In Scenario 1, all the weights were identical so sorting had no effect, and the three Options were effectively identical. For Scenarios 2 and 3, reproduction based on the parental weights led to positive and negative correlations in reproductive success over time for Options 2 and 3, respectively, but with slightly different magnitudes than obtained with the negative-binomial approach.

Tracking genetic drift

Table 2 illustrates how lifetime $V_{k\bullet}$ was calculated from simulated demographic data. To determine whether Hill's N_e based on these $V_{k\bullet}$ values accurately predicted the rate of genetic drift, two common genetic metrics were monitored. The expected variance in allele frequency ($V_{p(t)}$) after t generations of genetic drift is (Hedrick 2000):

$$E\left(V_{p(t)}\right) = p_0(1-p_0)\left[1-\left(1-\frac{1}{2N_e}\right)^t\right], \quad (4)$$

where p_0 is the initial allele frequency. In isolated populations with no mutation, random changes in allele frequency also cause an increase in homozygosity over time, such that after *t* generations the expected amount of remaining heterozygosity (H_t) is a simple function of initial average heterozygosity (H_0) and N_e (Crow and Kimura 1970):

$$H_t = H_0\left[1-\left(1-\frac{1}{2N_e}\right)^t\right]. \quad (5)$$

To monitor these metrics, genetic variation was tracked at *L* unlinked, diallelic (~SNP) loci. Genotypes were recorded as [0,1,2], indicating the number of copies of the focal allele each individual carried. In each replicate simulation, the population was initialized by filling each age class with the appropriate number (N_x) of individuals. In year 0, all individuals were designated as heterozygotes (genotype '1') at every locus, so initial allele frequencies were all $p_0 = 0.5$. In year 1 and subsequent years, mean observed H_t and $V_{p(t)}$ were computed for all members of the newborn cohort. As a single episode of random mating is sufficient to establish Hardy-Weinberg genotypic ratios, mean *H* at year 1 was on average 0.5. Years were converted into generations using the relationship $t=y/T$, where *y* is elapsed time in years (*T* = generation length was 4.84 for Scenario 1 and 5.22 for the other scenarios where male fecundity increased with age.)

Observed rates of genetic drift were compared with expected rates calculated two ways. Under the Hill-Felsenstein inference model, where probabilities of reproduction and survival are assumed to be independent over time (in agreement with Option 1 as implemented here), the expected variance in *LRS* and hence Hill's N_e can be calculated from an expanded life table (age-specific survival, fecundity, and ϕ) using the AgeNe model (Waples et al. 2011). The resulting N_e was then used in Equations 4 and 5 to generate expected values for the two genetic drift indices. The second approach used the population pedigree from the simulations to calculate $V_{k\bullet}$ for each annual cohort of offspring, and from this a 'pedigree' N_e was calculated every year using Equation 1. The harmonic mean pedigree N_e was then used in Equations 4 and 5 to predict expected rates of genetic drift based on the actual population pedigree.

With age structure, the rate of increase in $V_{p(t)}$ reaches a steady state only after a burnin period lasting several generations, which means that Equation 4 might not be accurate in the early years. To account for this effect, an adjustment factor *C* was calculated as the mean

difference between observed and expected $V_{p(t)}$ in years 30-50, shortly after the burnin period. Subsequent values of observed $V_{p(t)}$ were adjusted by subtracting C (see Figure S1). Each replicate simulation was run for 500 years. Except as noted, results shown here are averaged across 10 replicate simulations, each tracking genetic variation at L=100 loci.

RESULTS

Option 1

Population demography

Option 1 implements the inference model of Felsenstein (1971) and Hill (1972), where reproduction and survival are independent over time. For this Option, analytical expectations for lifetime $V_{k\bullet}$ and N_e under Hill's model are possible based on the vital rates in Table 1, and these provide a useful reference point for evaluating results of the simulations. Scenario 1 is the simplest as fecundity is constant in both sexes, with ϕ=1 for all ages. This means that all adults reproducing each year behave like a single Wright-Fisher population with Poisson variation in reproductive success. Under this Scenario, the parametric expectation for $V_{k\bullet}$ is 10.2 (Table 3). Poisson variance in *LRS* would lead to $V_{k\bullet}$ equal to the mean (which must be $\bar{k}\bullet = 2$ in a stable population), so most of the total lifetime variance can be attributed to variation in longevity (some individuals live longer than others and have more opportunities to reproduce). In Scenario 2, male fecundity increases with age, and at each age the variance in male offspring number is 5 times the mean (ϕ=5). Together these factors increase parametric $V_{k\bullet}$ to 16.1 (Table 3). In Scenario 3, ϕ takes a rather extreme value of 20, and parametric $V_{k\bullet}$ grows to 31.1 – over 15 times the lifetime mean.

These demographic changes have predictable consequences for effective population size under Option 1. In Scenario 1, where both sexes have identical vital rates (leading to T=4.84 and $V_{k\bullet} = 10.2$), parametric N_e from Equation 1 is 4*400*4.84/(2+10.18) = 636. In Scenarios 2 and 3, increasing fecundity with age increased generation length in males from 4.84 to 5.59, so across both sexes overall T was 5.21. All else being equal, N_e increases linearly with generation length (Equation 1). However, oversdispersion in male reproductive success substantially increased in Scenarios 2 and 3, and this more than offset the modest increase in generation

length. The parametric expectations for N_e are 452 for Scenario 2 and 253 for Scenario 3 (Table 3), which are, respectively, 29% and 60% lower than for Scenario 1.

The new correlation metric, $\rho_{\alpha,\alpha+}$, examines the association between an individual's reproductive success in the first year of sexual maturity (age 3 for the core life table) and the rest of its life. As expected under Option 1, mean values of $\rho_{\alpha,\alpha+}$ for both sexes for all three scenarios were close to zero, all falling in the range [-0.01, +0.01] (data not shown).

For both of the algorithms for modeling reproduction, mean empirical $V_{k\bullet}$ in the simulations agreed well with the parametric expectations (Figure 1). Harmonic mean N_e calculated from the simulated pedigrees was slightly (~1%) higher than the parametric expectation for Scenarios 1 and 2 and 4-7% higher for Scenario 3 (Table 3). This latter result reflects the difficulty in precisely modeling strongly overdispersed variance in reproductive success, especially when older age classes can have few individuals (only 8 of each sex for age 10 in the core life table).

Tracking genetic drift

For all 3 Scenarios under Option 1, and for both algorithms of simulating reproduction, the mean ratio of observed to expected heterozygosity calculated over the last 50 years of each replicate was close to unity (all values within 1% of 1.0; Table 3). A comparable result was found for comparisons of observed and expected variance in allele frequency (Table S2). These results are consistent with but extend previously reported results for Hill's model. Waples et al. (2014) found excellent agreement between observed and expected rates of decline in heterozygosity in simulations based on vital rates for 20 different species, but for most species it was assumed that ϕ=1 for all ages. Results for Scenario 3, with very high within-age reproductive skew (ϕ=20), are therefore new.

Options 2 and 3

Population demography

As expected, for Scenario 1 results were qualitatively different for the two algorithms. With ϕ=1, parental weights are all the same, so $V_{k\bullet}$ (Figure 1) and pedigree N_e and $\rho_{\alpha,\alpha+}$ (Table 3) were essentially identical for Options 1-3 for *THEWEIGHT*. In *NEGBINOM*, the realized offspring numbers each year were sorted in Option 2 and 3; although these realized annual offspring

numbers spanned a relatively small range of values for Scenario 1, when sorted before assigning to individuals these had a substantial effect on population demography. Using *NEGBINOM* for Scenario 1, $V_{k\bullet}$ more than doubled under Option 2 and was nearly halved under Option 3 (Figure 1), with corresponding changes to pedigree N_e (Table 3), and $\rho_{\alpha,\alpha+}$ was strongly positive in both sexes (0.85) for Option 2 and strongly negative in both sexes (-0.68 to -0.69) for Option 3 (Table 3).

Under Scenarios 2 and 3, results were even more dramatic. For Option 2, $\rho_{\alpha,\alpha+}$ was >0.9 for both algorithms (Table 3). These strong positive correlations concentrated reproduction in a relatively few individuals, which in turn substantially increased lifetime variance in reproductive success. With ϕ=5 (Scenario 2), lifetime $V_{k\bullet}$ increased almost four-fold, and with ϕ=20 (Scenario 3), $V_{k\bullet}$ more than quadrupled, to >200 for both algorithms (Figure 1). Increases in $V_{k\bullet}$ caused corresponding decreases in effective size under Option 2 (Table 3). For Scenario 2, N_e was less than half of the parametric value expected under Option 1 for both algorithms, and for Scenario 3 realized N_e was less than 30% of the value expected if population demography had followed the assumptions of Hill's model.

In Option 3, individuals who were assigned the largest numbers of offspring each year (*NEGBINOM*) or were assigned the largest parental weights (*THEWEIGHT*) all died before reaching the next age. This created a strong negative correlation between initial and subsequent reproductive success for both algorithms: $\rho_{\alpha,\alpha+}$ = -0.34 to -0.37 for Scenario 2 and -0.09 to -0.11 for Scenario 3 (Table 3). These negative correlations minimized disparities in lifetime reproductive success and reduced $V_{k\bullet}$ compared to expectations under the Hill model (Figure 1) and consequently increased effective size (Table 3).

Tracking genetic drift

In spite of the fact that Options 2 and 3 implemented extreme violations of assumptions of Hill's model, use of the harmonic mean pedigree N_e in Hill's Equation 1 accurately predicted the rates of loss of heterozygosity and increase in allele frequency variance (Tables 3 and S2; Figures 2 and 3). For loss of heterozygosity, all deviations from expectations were <1% except for the extremely overdispersed (ϕ =20) Scenario 3 under Option 2, where mean heterozygosity in the last 50 years was 1.5% higher than expected using *NEGBINOM* and 2.1% higher using *THEWEIGHT* (Table 3). Stochastic variation in the rate of increase in allele frequency variance

was somewhat higher, but for most Scenario x Option combinations the observed change in $V_{p(t)}$ was within 1% of the expected (Table S2), with 3 scenarios involving overdispersed variance (ϕ =5 or 20) being 2-4% higher or lower than expected.

Alternate life histories

Results so far have all used variations of the vital rates in Table 1, which apply to a hypothetical species with 10 age classes. Simulations were also conducted for shorter lifespans (5 years, with age at maturity 1) and longer lifespans (20 years, with age at maturity 5) (Table S3). In both cases, fecundity was constant with ϕ=1 in females, and fecundity was proportional to age with ϕ=5 in males. As shown in Figure S2, Equation 1 based on N_e calculated from the actual pedigrees accurately predicted the rates of loss of heterozygosity and increase in allele frequency variance for these different life histories.

Precision

As the main focus of this paper is to evaluate potential bias in Equation 1 when it is applied to scenarios that dramatically violate assumptions of the inference model used in its derivation, a great deal of replication has been used to smooth out random demographic and genetic stochasticity to produce results that are qualitatively repeatable. Empirical datasets, on the other hand, generally are collected from a single realized population pedigree and might include data for a relatively small number of genes. As a reminder to researchers evaluating such empirical datasets, an example is included that generated a single 500-year population pedigree and tracked decline of heterozygosity in 10 different sets of 50 unlinked diallelic loci (Figure 4). At year 500 the average heterozygosity across the total 500 loci was close to the expected value from Equation 5 using the realized pedigree (0.256), but in one set of 50 loci mean (H_{obs}) was >0.3 and in another set it was <0.2. Comparable results for allele frequency variance are shown in Figure 1 of Waples (2022b).

DISCUSSION

Although sensitivity of models to underlying assumptions can vary widely, there is no shortage of examples from ecology and evolutionary biology where discrepancy between assumptions and reality can lead to substantial bias. A classic example is Wright's (1931 and

later) famous equation relating F_{ST} to the product of migration rate (m) and effective population size: $F_{ST} \approx 1/(1+4mN_e)$. This relationship was derived for Wright's island model, which makes a number of convenient but unrealistic assumptions about patterns of migration and constancy of subpopulation sizes. Under more realistic assumptions, this relationship can be quite different (Whitlock and McCauley 1999; Nunney 1999). Some more recent examples of effects of violating model assumptions include the demonstrations that a) unaccounted-for spatial structure can bias both stock assessment models (Punt 2019) and close-kin mark recapture models to estimate abundance (Conn et al. 2020); b) species boundaries under the multispecies coalescent are sensitive to model assumptions involving spatial structure, migration, and changes in abundance (Barley et al 2018); and c) phylogenetic inferences are sensitive to the common assumption that the data have evolved under stationary, reversible, and homogeneous conditions (Naser-Khdour et al. 2021).

In stark contrast to these results, Hill's (1972) method for calculating effective population size is surprisingly robust to extreme violations of the assumptions he made in deriving his analytical results. Two general kinds of assumptions underpin Hill's model: 1) the population's size and age structure are stable; 2) an individual's reproduction in one time period has no effect on its future reproduction or survival. Previous work has demonstrated that Hill's model is robust to fluctuations in abundance and age structure arising from random demographic stochasticity, so focus here was on the second set of assumptions. As expected, introducing strong autocorrelations in reproduction and covariance between reproduction and survival caused dramatic changes in lifetime variance in reproductive success. For Scenario 1 using the *NEGBINOM* algorithm, mean $V_{k\bullet}$ was 3.8 times as large under Option 2 (positive autocorrelations and covariances) as it was under Option 3 (negative autocorrelations and covariances). For Scenarios 2 and 3, which included substantial overdispersion of within-age reproductive success, the proportional differences were even greater (7.7 and 6.4 times larger for Option 2, respectively, using results averaged across both algorithms). The autocorrelations and covariances that arose when implementing Options 2 and 3 did not affect generation length, so when the empirically-derived estimates of $V_{k\bullet}$ were inserted in Hill's Equation 1, they also led to realized effective sizes that differed dramatically among the three Options (Table 3).

The most surprising result from this study is that, although Hill's model assumed no autocorrelations or covariances, when $V_{k\bullet}$ is computed from the population pedigree, N_e

calculated from Equation 1 accurately predicts the realized rate of genetic drift when inserted in Equations 4 (for rate of increase in allele frequency variance) and 5 (for rate of loss of heterozygosity). Excellent agreement between observed and predicted rates of genetic drift was found for diverse life histories (5, 10, and 20 year lifespans, with age at maturity 1, 3, or 5 years), for identical or different vital rates for males and females, and for extreme skew in reproductive success (variance up to 20 times the mean), all across nearly 100 generations of evolution.

These results are good news for researchers. Random processes in age-structured populations create dynamic heterogeneity in survival and reproduction (Vindenes et al. 2008; Tuljapurkar et al. 2009), and these processes are consistent with Hill's model and are implemented here as Option 1. But the biological attributes of many species create autocorrelations of reproduction and/or covariances in reproduction and survival that violate core assumptions of Hill's model. As implemented here, Options 2 and 3 are more extreme than are likely to be found in most real species, but that was intentional. In the worst-case scenarios found here, observed rates of genetic drift were still within a few percent of those expected, and these scenarios involved very strong reproductive skew within ages. For all realistic applications to natural populations, therefore, Equation 1 can be considered to be a very reliable predictor of effective population size.

The two algorithms for modeling reproduction were equally successful in achieving the desired level of reproductive skew under Option 1, for which an analytical expectation is possible: excellent agreement was found between observed and expected $V_{k\bullet}$ for all three Scenarios (Figure 1). As expected, under Scenario 1 results for *THEWEIGHT* did not vary across the three Options, whereas those for *NEGBINOM* did. For Scenarios 2 and 3, which involved moderately high or very high reproductive skew among individuals of the same age, the two algorithms produced qualitatively similar patters with some quantitative differences. Two factors contributed to these relatively modest differences. First, whereas in *NEGBINOM* the vectors of randomly-generated offspring numbers were sorted before assigning to individuals, in *THEWEIGHT* what was sorted were randomly-generated parental weights, which only represent relative probabilities of producing offspring, not actual offspring numbers. The second factor is that when reproductive skew is very high (ϕ =20 in Scenario 3), most randomly-generated weights, and most randomly-generated offspring numbers, will be 0. As discussed by Waples (2022a), this creates some challenges when modeling age-structured populations of long-lived

species, for which the numbers of individuals in older age classes can be very small (in the core lifetable in Table 1, there are only 8 age-10 individuals of each sex).

Although pairwise correlations of individual reproductive success in different years can provide valuable and detailed information regarding reproductive tradeoffs, the new index introduced here ($\rho_{\alpha,\alpha+}$) provides what appears to be a robust summary across the full lifespan. $\rho_{\alpha,\alpha+}$ is the correlation between two vectors, one listing the number of offspring produced by each individual at the first age of sexual maturity (α) and the other listing the total number of offspring produced by the same individuals during the rest of their lifetimes. As expected under Hill's inference model, these correlations averaged close to 0 under Option 1 and were consistently very high under Option 2. Under Option 3 these average correlations were consistently negative, with a magnitude that depended on the degree of within-age reproductive skew. An advantage of this summary index compared to pairwise correlations of reproduction at specific ages is that the length of the two vectors considered by $\rho_{\alpha,\alpha+}$ is the number of individuals in the cohort, rather than the inevitably smaller (and variable) number that survive to later ages. This increases statistical power, so $\rho_{\alpha,\alpha+}$ might be used initially for diagnostic purposes before focusing in more detail on specific ages.

ACKNOWLEDGEMENTS

The author is grateful to Bill Hill for many insightful discussions over the years, relating to effective population size as well as other topics.

Data archiving

All results presented here were generated by simulations. R code to conduct simulations for the NegBinom algorithm is available in Supporting Information, and all code will be deposited on Zenodo on acceptance. The author declares no conflict of interest.

REFERENCES

Barley, A.J., Brown, J.M. and Thomson, R.C., 2018. Impact of model violations on the inference of species boundaries under the multispecies coalescent. *Systematic Biology*, *67*(2), pp.269-284.

Bell, G., 1980. The costs of reproduction and their consequences. *The American Naturalist*, *116*(1), pp.45-76.

Byholm, P., A. Nikula, J. Kentta, and J.-P. Taivalmäki. 2007. Interactions between habitat heterogeneity and food affect reproductive output in a top predator. Journal of Animal Ecology 76:392–401.

Caswell, H. (2001). Matrix Population Models: Construction, Analysis, and Interpretation, 2nd edn. Sinauer Associates, Sunderland, MA.

Charlesworth, B., 1994. *Evolution in age-structured populations*. Second Edition. Cambridge: Cambridge University Press.

Conn, P. B., Bravington, M. V., Baylis, S., & Ver Hoef, J. M. (2020). Robustness of close-kin mark–recapture estimators to dispersal limitation and spatially varying sampling probabilities. *Ecology and Evolution*, *10*, 5558–5569.

Crow, J.F. and Kimura, M. 1970. *An introduction in population genetics theory*. New York (NY): Harper and Row.

Cushing, J.M., 1994. The dynamics of hierarchical age-structured populations. *Journal of Mathematical Biology*, *32*, pp.705-729.

Felsenstein J. 1971. Inbreeding and variance effective numbers in populations with overlapping generations. Genetics. 68:581–597.

Hedrick PW. 2000. Genetics of populations. 2nd ed. Sudbury (MA): Jones and Bartlett.

Hill, W.G., 1972 Effective size of population with overlapping generations. *Theoretical Population Biology* 3: 278–289.

Kruuk, L.E., 2004. Estimating genetic parameters in natural populations using the 'animal model'. *Philosophical Transactions of the Royal Society of London. Series B: Biological Sciences*, *359*(1446), pp.873-890.

Lande, R., Engen, S. and Saether, B.E., 2003. *Stochastic population dynamics in ecology and conservation*. Oxford University Press.

Lee, A.M., S. Engen, & B.-E. Sæther, (2011) The influence of persistent individual differences and age at maturity on effective population size. *Proceedings of the Royal Society of London, Series B: Biological Sciences*, 278, 3303-3312.

Lee, A.M., Myhre, A.M., Markussen, S.S., Engen, S., Solberg, E.J., Haanes, H., Røed, K., Herfindal, I., Heim, M. and Sæther, B.E., 2020. Decomposing demographic contributions to the effective population size with moose as a case study. *Molecular ecology*, *29*(1), pp.56-70.

McElligott, A.G. and Hayden, T.J., 2000. Lifetime mating success, sexual selection and life history of fallow bucks (Dama dama). *Behavioral Ecology and Sociobiology*, *48*, pp.203-210.

Mousseau, T. A., and C. W. Fox, eds. 1998. Maternal effects as adaptations. Oxford University Press, New York.

Naser-Khdour, S., Minh, B.Q. and Lanfear, R., 2021. The influence of model violation on phylogenetic inference: a simulation study. *bioRxiv*, pp.2021-09.

Nunney, L., 1999. The effective size of a hierarchically structured population. *Evolution*, *53*(1), pp.1-10.
Pelletier, F., Hogg, J.T. and Festa-Bianchet, M., 2006. Male mating effort in a polygynous ungulate. *Behavioral Ecology and Sociobiology*, *60*, pp.645-654.
Punt, A.E., 2019. Spatial stock assessment methods: a viewpoint on current issues and assumptions. *Fisheries Research*, *213*, pp.132-143.
R Core Team (2021). R: A language and environment for statistical computing. R Foundation for Statistical Computing, Vienna, Austria. URL https://www.R-project.org/
Reznick, D., 1992. Measuring the costs of reproduction. *Trends in ecology & evolution*, *7*(2), pp.42-45.
Roff, D. 1992. *Evolution of life histories: theory and analysis*. Chapman and Hall, New York.
Smith, J.N., 1981. Does high fecundity reduce survival in song sparrows?. *Evolution*, pp.1142-1148.
Tuljapurkar, S., Steiner, U.K. and Orzack, S.H., 2009. Dynamic heterogeneity in life histories. *Ecology letters*, *12*(1), pp.93-106.
Van Noordwijk, A.J. and De Jong, G., 1986. Acquisition and allocation of resources: their influence on variation in life history tactics. *The American Naturalist*, *128*(1), pp.137-142.
Vindenes, Y., Engen, S. and Sæther, B.E., 2008. Individual heterogeneity in vital parameters and demographic stochasticity. *The American Naturalist*, *171*(4), pp.455-467.
Waples, R.S. 2020. An estimator of the Opportunity for Selection that is independent of mean fitness. Evolution 74:1942-1953.
Waples, RS. 2022a. *TheWeight*: A simple and flexible algorithm for simulating non-ideal, age-structured populations. Methods in Ecology and Evolution 13:2030-2041.
Waples, RS. 2022b. What is N_e, anyway? Journal of Heredity 113:371-379.
Waples, R.S., C. Do, and J. Chopelet. 2011. Calculating N_e and N_e/N in age-structured populations: a hybrid Felsenstein-Hill approach. Ecology 92:1513-1522.
Waples, R.S., T. Antao, and G. Luikart. 2014. Effects of overlapping generations on linkage disequilibrium estimates of effective population size. Genetics 197:769-780.
Waples, RS, and P Feutry. 2022. Close-kin methods to estimate census size and effective population size. Fish and Fisheries 23:273-293.
Whitlock, M.C. and McCauley, D.E., 1999. Indirect measures of gene flow and migration: FST≠ 1/(4Nm+1). *Heredity*, *82*(2), pp.117-125.
Williams, G.C., 1966. Natural selection, the costs of reproduction, and a refinement of Lack's principle. *The American Naturalist*, *100*(916), pp.687-690.
Wilson, A.J. and Nussey, D.H., 2010. What is individual quality? An evolutionary perspective. *Trends in ecology & evolution*, *25*(4), pp.207-214.
Wright, S., 1931. Evolution in Mendelian populations. *Genetics*, *16*(2), p.97-159.
Wright, S., 1938. Size of population and breeding structure in relation to evolution. *Science*, *87*, pp.430-431.

Table 1. Core vital rates used in the simulations. The hypothetical population matures at age 3 and has a maximum age of 10. Survival is constant at s_x = 0.7/year, and the vector N_x is the number of individuals of each sex in each age class. In females, fecundity (b_x) is always constant with age, and within each age the distribution of offspring number is Poisson (ϕ=1). In Scenario 1, male vital rates are identical to those for females. In Scenarios 2 and 3, male fecundity increases with age, and within ages reproductive variance is either substantially overdispersed (ϕ=5; Scenario 2) or very strongly overdispersed (ϕ=20; Scenario 3). Fecundity is scaled to values that will produce a stable population. Table S3 shows vital rates for some other life histories that were modeled.

					Male					
			Female		Scenario 1		Scenario 2		Scenario 3	
Age	N_x	s_x	b_x	ϕ_x	b_x	ϕ_x	b_x	ϕ_x	b_x	ϕ_x
1	200	0.7	0	0	0	0	0	0	0	0
2	140	0.7	0	0	0	0	0	0	0	0
3	98	0.7	1.30	1	1.30	1	0.80	5	0.80	20
4	69	0.7	1.30	1	1.30	1	1.07	5	1.07	20
5	48	0.7	1.30	1	1.30	1	1.34	5	1.34	20
6	34	0.7	1.30	1	1.30	1	1.61	5	1.61	20
7	24	0.7	1.30	1	1.30	1	1.88	5	1.88	20
8	16	0.7	1.30	1	1.30	1	2.15	5	2.15	20
9	12	0.7	1.30	1	1.30	1	2.41	5	2.41	20
10	8	0	1.30	1	1.30	1	2.68	5	2.68	20

Table 2. Example illustrating how positive correlations in reproductive success over time were generated in simulated populations. For each of 20 individuals in a cohort, the number of offspring produced at each age 1-5 is shown in the left table. Each year individuals with the highest ID numbers die, after which time their reproductive success is recorded as NA. In the left set of columns, offspring numbers were randomly generated for survivors at each age, as occurs under Option 1; in the right set of columns, those random numbers were sorted so that each year the individual with the lowest ID produced the most offspring (as occurs in Option 2). The columns labeled '*LRS*' show the total lifetime numbers of offspring produced by each individual, and the columns labeled '*LRS*-' show *LRS* for all ages except age 1. See text for discussion and Table S1 for an example illustrating Option 3.

	Option 1							Option 2						
	Age							Age						
ID	1	2	3	4	5	*LRS*	*LRS-*	1	2	3	4	5	*LRS*	*LRS-*
1	6	5	1	1	4	17	11	6	17	8	8	4	43	37
2	0	1	0	6	4	11	11	5	5	7	6	4	27	22
3	0	1	2	1	NA	4	4	3	2	3	5	NA	13	10
4	1	0	0	8	NA	9	8	2	1	2	1	NA	6	4
5	1	17	8	5	NA	31	30	1	1	1	1	NA	4	3
6	0	0	0	NA	NA	0	0	1	1	0	NA	NA	2	1
7	0	0	7	NA	NA	7	7	0	1	0	NA	NA	1	1
8	0	0	3	NA	NA	3	3	0	1	0	NA	NA	1	1
9	0	1	NA	NA	NA	1	1	0	0	NA	NA	NA	0	0
10	0	2	NA	NA	NA	2	2	0	0	NA	NA	NA	0	0
11	2	1	NA	NA	NA	3	1	0	0	NA	NA	NA	0	0
12	0	1	NA	NA	NA	1	1	0	0	NA	NA	NA	0	0
13	0	NA	NA	NA	NA	0	0	0	NA	NA	NA	NA	0	0
14	0	NA	NA	NA	NA	0	0	0	NA	NA	NA	NA	0	0
15	5	NA	NA	NA	NA	5	0	0	NA	NA	NA	NA	0	0
16	0	NA	NA	NA	NA	0	0	0	NA	NA	NA	NA	0	0
17	3	NA	NA	NA	NA	3	0	0	NA	NA	NA	NA	0	0
18	0	NA	NA	NA	NA	0	0	0	NA	NA	NA	NA	0	0
19	0	NA	NA	NA	NA	0	0	0	NA	NA	NA	NA	0	0
20	0	NA	NA	NA	NA	0	0	0	NA	NA	NA	NA	0	0

Table 3. Summary of simulation results for the two algorithms for modeling reproduction, for the three Scenarios (1→ϕ=1; 2→ϕ=5; 3→ϕ=20). For each Scenario, the parametric $V_{k\bullet}$ and N_e under Hill's model (here implemented as Option 1) are shown. Columns on the left show the N_e calculated from the simulated pedigrees; middle columns show the ratio of observed heterozygosity to expected heterozygosity based on the pedigree N_e; columns on the right show the correlation ($\rho_{\alpha,\alpha+}$) between offspring numbers for each individual at age α and for all subsequent ages combined (as shown in the *LRS*- column from Table 2). Pedigree N_e was calculated as the harmonic mean across cohorts and replicates; the ratio H_{obs}/H_{exp} was the average across 10 replicates, and within each replicate the ratio was calculated as the mean across the final 50 years. For each cohort in each replicate, $\rho_{\alpha,\alpha+}$ was computed across all individuals that reached age at maturity, and results were averaged across cohorts and replicates. See Table S2 for comparison of observed and expected rates on increase in allele frequency variance, $V_{p(t)}$.

			Pedigree N_e			H_{obs}/H_{exp}			Correlation ($\rho_{\alpha,\alpha+}$)			
	Option 1		Option			Option			Option 2		Option 3	
Scenario	E($V_{k\bullet}$)	E(N_e)	1	2	3	1	2	3	F	M	F	M
NegBin												
1	10.2	636	640	324	999	0.999	1.007	1.003	0.85	0.85	-0.68	-0.69
2	16.1	462	468	159	795	0.999	1.008	0.999		0.94		-0.34
3	31.1	253	270	72	367	0.996	1.015	0.999		0.94		-0.11
THEWEIGHT												
1[a]	10.2	636	640	640	639	1.001	1.001	0.999	0.001	-0.006	-0.006	0.004
2	16.1	462	468	201	673	1.007	0.994	1.003		0.91		-0.37
3	31.1	253	263	65	329	0.998	1.021	0.999		0.90		-0.09

[a] Note that under Scenario 1 for *TheWeight*, all parental weights are equal, so sorting the weights has no effect and Options 2 and 3 become effectively identical.

Figure Legends

Figure 1. Mean values of the lifetime variance in reproductive success ($V_{k\bullet}$) for simulated data using two algorithms for controlling reproduction (*NEGBIN*, dotted blue lines and blue symbols; and *THEWEIGHT*, dashed red lines and red symbols). Results are shown for the three Options and three Scenarios described in the text. Parametric expectations based on the vital rates in Table 1, which are only available for Option 1, are shown by black Xs. Note the log scale on the Y axis. Under Scenario 1 for *THEWEIGHT*, all parental weights are equal so sorting the weights has no effect and Options 2 and 3 become effectively identical.

Figure 2. Observed (colored symbols) and expected (black lines) rates of genetic drift in a simulated population under Option 2, Scenario 2 (in which ϕ=5 for all ages in males). The left Y axis and red symbols plot loss of heterozygosity and the right Y axis and cyan symbols plot increasing variance in allele frequency. Expected rates of genetic drift were computed using Equations 4 and 5 and the harmonic mean pedigree N_e for this scenario (which was 158 using the negative binomial method). Results shown are averaged across 10 replicate 500-year pedigrees, each of which tracked genetic variation at 100 unlinked, diallelic loci.

Figure 3. Observed (colored symbols) and expected (black lines) rates of loss of heterozygosity in simulated populations for three Options that lead to positive correlations (Option 2), negative correlations (Option 3), and independence of individual reproductive success over time (Option 1). These results are for the negative binomial method under Scenario 3, in which ϕ = 20 for males of all ages. Results shown are averaged across 10 replicate 500-year pedigrees, each of which tracked genetic variation at 100 unlinked, diallelic loci.

Figure 4. Observed (colored lines) and expected (solid black line) decline in observed heterozygosity for 10 different sets of 50 diallelic loci tracked on a single, 500-year pedigree. These results are for the negative binomial algorithm under Option 2 and Scenario 3, in which ϕ = 20 for males of all ages.

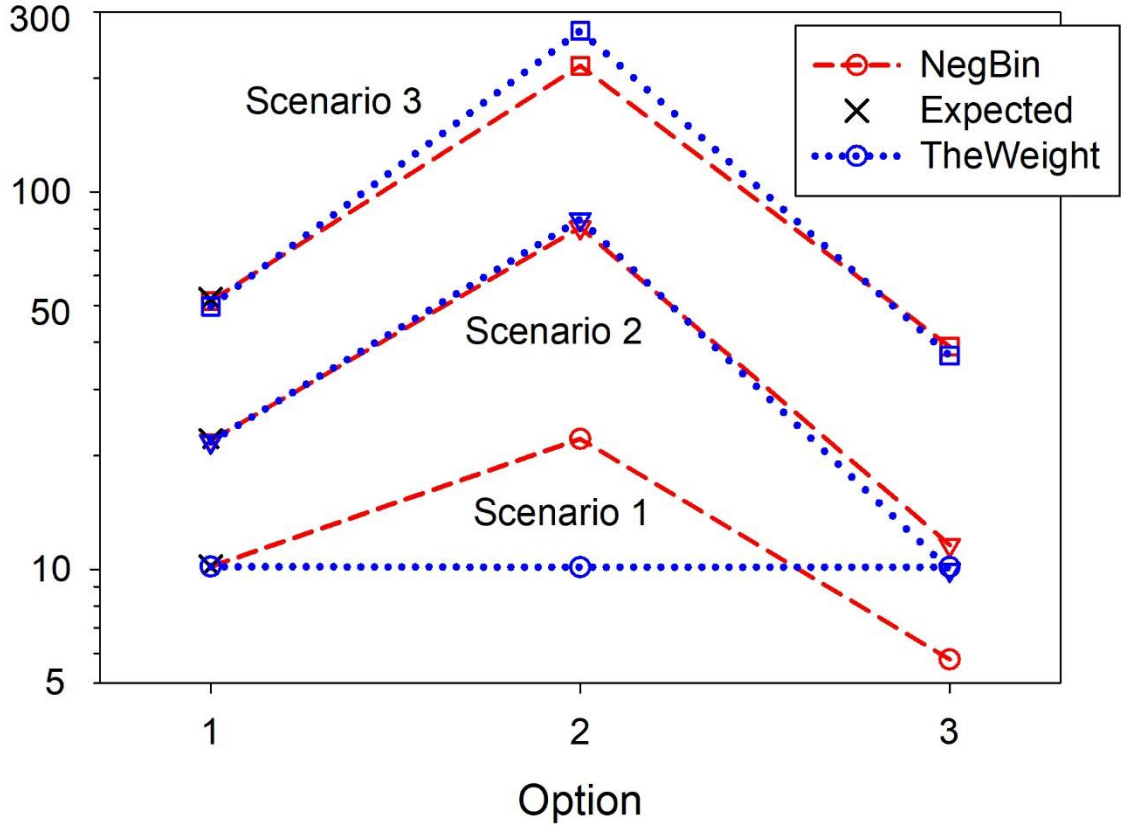

Figure 1. Mean values of the lifetime variance in reproductive success ($V_{k\bullet}$) for simulated data using two algorithms for controlling reproduction (*NEGBIN*, dotted blue lines and blue symbols; and *THEWEIGHT*, dashed red lines and red symbols). Results are shown for the three Options and three Scenarios described in the text. Parametric expectations based on the vital rates in Table 1, which are only available for Option 1, are shown by black Xs. Note the log scale on the Y axis. Under Scenario 1 for *THEWEIGHT*, all parental weights are equal so sorting the weights has no effect and Options 2 and 3 become effectively identical.

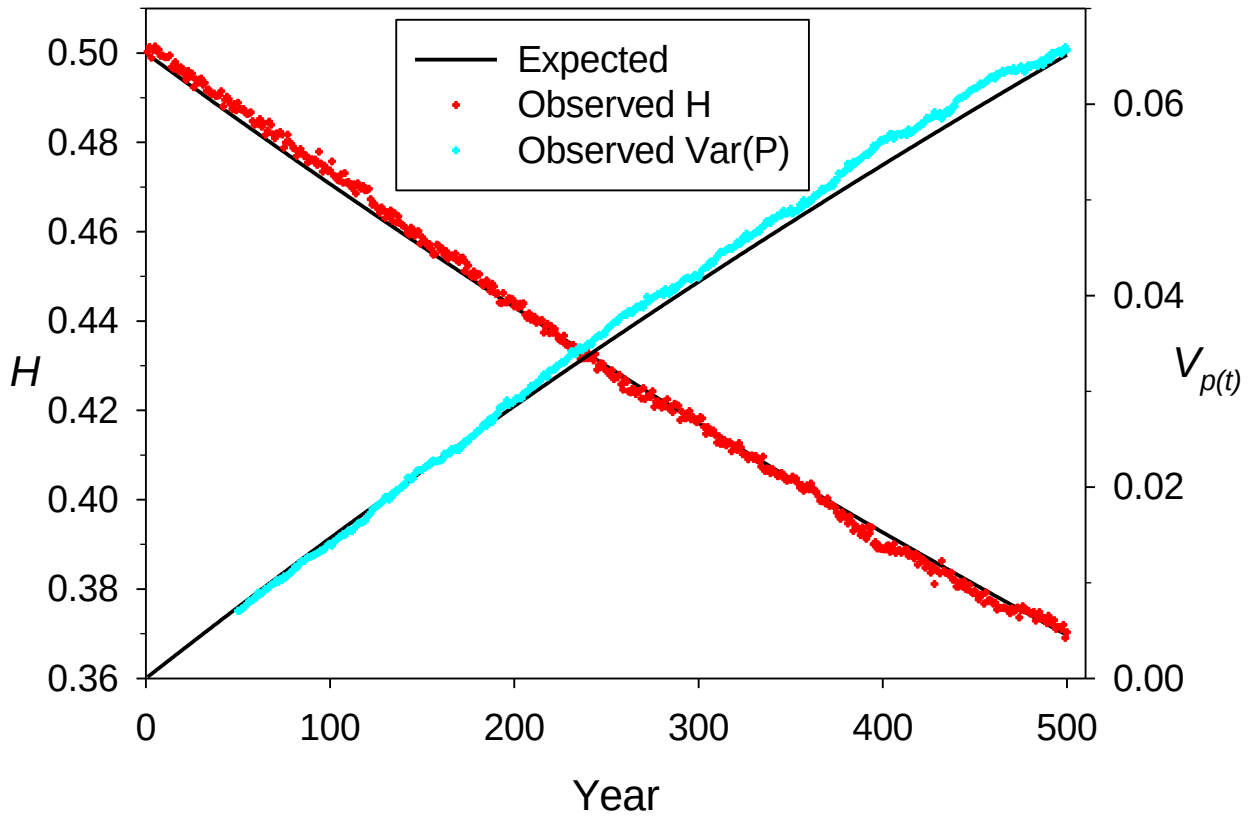

Figure 2. Observed (colored symbols) and expected (black lines) rates of genetic drift in a simulated population under Option 2, Scenario 2 (in which ϕ=5 for all ages in males). The left Y axis and red symbols plot loss of heterozygosity and the right Y axis and cyan symbols plot increasing variance in allele frequency. Expected rates of genetic drift were computed using Equations 4 and 5 and the harmonic mean pedigree N_e for this scenario (which was 158 using the negative binomial method). Results shown are averaged across 10 replicate 500-year pedigrees, each of which tracked genetic variation at 100 unlinked, diallelic loci.

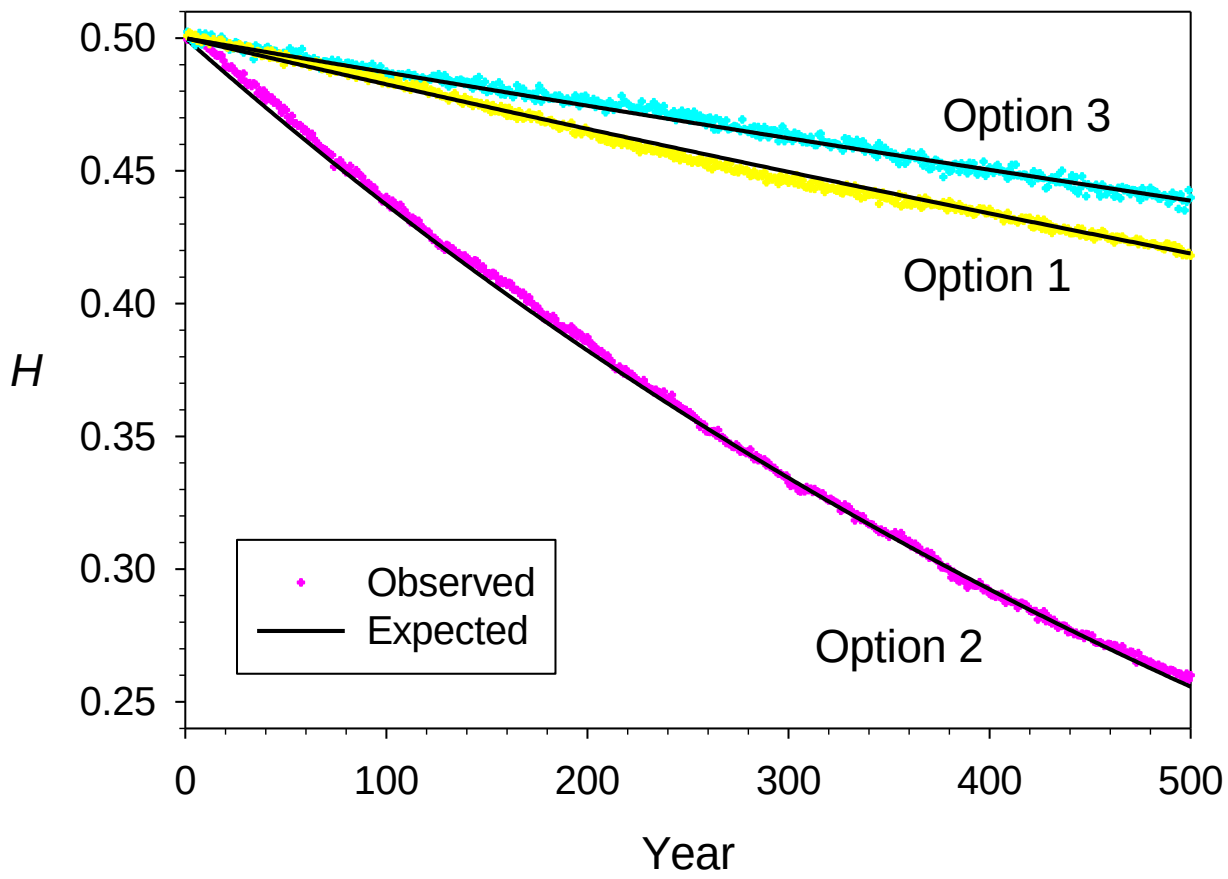

Figure 3. Observed (colored symbols) and expected (black lines) rates of loss of heterozygosity in simulated populations for three Options that lead to positive correlations (Option 2), negative correlations (Option 3), and independence of individual reproductive success over time (Option 1). These results are for the negative binomial method under Scenario 3, in which $\phi = 20$ for males of all ages. Results shown are averaged across 10 replicate 500-year pedigrees, each of which tracked genetic variation at 100 unlinked, diallelic loci.

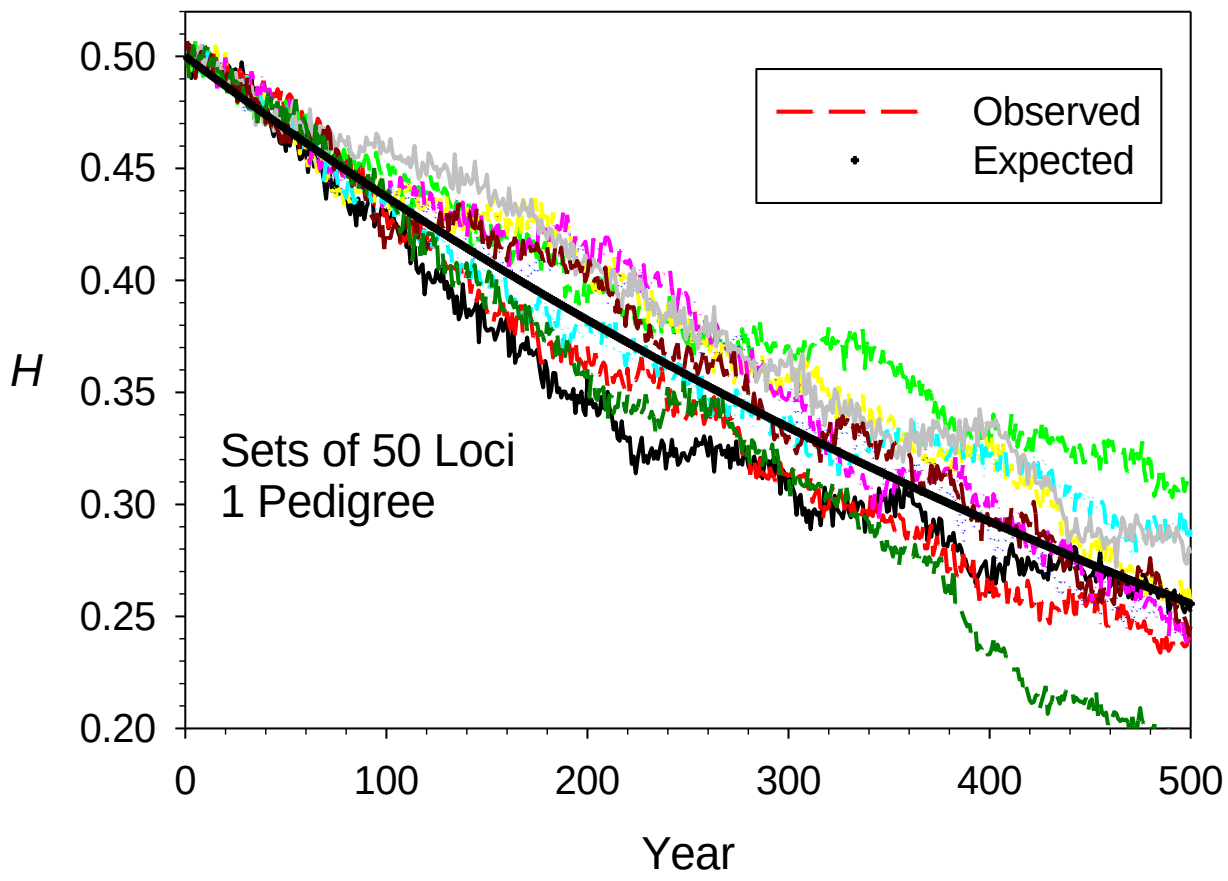

Figure 4. Observed (colored lines) and expected (solid black line) decline in observed heterozygosity for 10 different sets of 50 diallelic loci tracked on a single, 500-year pedigree. These results are for the negative binomial algorithm under Option 2 and Scenario 3, in which $\phi = 20$ for males of all ages.